Advanced Powder Technology 36 (2025) 105028

Contents lists available at ScienceDirect

Advanced Powder Technology

journal homepage: www.elsevier.com/locate/apt

Original Research Paper

Evaluating the effects of electrolytes on the interaction forces between alumina surfaces in polyacrylic acid solutions using atomic force microscopy

Naoto Kishimoto [a], Ryota Kaji [b], Katsumi Tsuchiya [b], Koreyoshi Imamura [a], Naoyuki Ishida [b,*]

[a] Graduate School of Natural Science and Technology, Okayama University, Okayama, Japan
[b] Faculty of Science and Engineering, Doshisha University, Kyoto, Japan

ARTICLE INFO

Article history:
Received 10 May 2025
Received in revised form 30 July 2025
Accepted 31 July 2025
Available online 23 August 2025

Keywords:
Interaction force
Alumina surface
Anionic polyelectrolyte
Coexisting electrolyte
Atomic force microscopy

ABSTRACT

Evaluation and control of ceramic slurry at the microscopic level are critical to ensure consistent quality in manufactured ceramics. Notably, metal ions such as Mg^{2+} and Al^{3+} are common in ceramic slurries and significantly influence the stability of particle. This study applied atomic force microscopy to investigate the interaction forces between alumina particle surfaces in the presence of different concentrations of three metal ions and polyacrylic acid (PAA), a widely used dispersant.

The attractive forces observed at low PAA concentrations were attributed to polymer bridging between alumina surfaces, whereas the repulsive forces observed at high PAA concentrations were attributed to the domination of steric repulsion between adsorbed PAA molecules. The presence of multivalent metal ions, such as Mg^{2+} and Al^{3+}, modulated these interactions; an increasing ion valence induced a transition from repulsive to attractive force, primarily owing to electrostatic screening, which caused conformational collapse of the PAA chains and diminished the range of steric repulsion. Similarly, increasing the concentration of these metal ions decreased the range of repulsive forces, eventually resulting in a net attraction driven by the same electrostatic and polymer conformation mechanisms. Notably, the addition of 0.1 M $AlCl_3$ produced an anomalous long-range attraction between surfaces that could not be explained by conventional mechanisms, such as polymer bridging or electrostatic interactions between charge domains.

1. Introduction

Particle suspensions, also known as slurries or particle dispersions, play a crucial role in many industrial processes. Recent rapid advances in nanotechnology have driven the adaptation of industrial processes for handling nanoscale materials, including nanoparticles, to harness their unique functionalities. Because these nanomaterials are often processed as dispersions in liquids, the precise control of dispersion properties, such as stability, sedimentation, and rheology, has become increasingly critical.

The wet forming of ceramics is a widely used industrial process that utilises particle dispersions. In this method, ceramic particles, such as titania or alumina, are dispersed in an aqueous solution to form a slurry, which is subsequently poured into moulds to achieve the desired shape, then dried and sintered to produce the final product. The fluidic properties of these slurries, which include viscosity and packing fraction, are significantly influenced by the particle dispersion/aggregation behaviour and are key determinants of final material characteristics, such as density, homogeneity, and resistance to cracking or chipping. Therefore, the precise evaluation and control of the slurry dispersion state at the microscopic level are essential for optimising the ceramic manufacturing process.

Generally, particle dispersion/aggregation is dominated by the interactions of forces acting between particle surfaces, which are determined by the properties of the liquid, surfaces, solutes, etc. Although the Derjaguin – Landau – Verwey – Overbeek (DLVO) theory [1,2] has long provided a theoretical basis for predicting the dispersion/aggregation behaviours of charged particles in aqueous solutions, the development of a method for directly measuring surface interaction forces using a surface force apparatus (SFA) [3] and atomic force microscopy (AFM) [4,5] has facilitated remarkable progress in understanding surface forces. One of the most significant achievements of such direct surface force mea-

* Corresponding author.
E-mail address: naishida@mail.doshisha.ac.jp (N. Ishida).

https://doi.org/10.1016/j.apt.2025.105028

surements was the identification of surface forces not described by DLVO theory, often called non-DLVO forces [6], that exert critical influences on the behaviours of particle suspensions.

The behaviours of particles in ceramic slurries are typically controlled by the addition of dispersants, such as charged polymers. Normally, the addition of an appropriate quantity of dispersant induces steric repulsion, a typical non-DLVO force, between particle surfaces owing to the steric hindrance of adsorbed molecules. Thus, the interaction forces between the particle surfaces in a dispersant solution are significantly affected by the adsorption properties of the dispersant and characteristics of the solution, which include the pH and presence of co-solutes. In ceramic slurries, the presence of multivalent metal ions, such as Mg^{2+} and Al^{3+}, which are often eluted from the particles or added as sintering aids in the slurry preparation process, is known to have a significant impact on their dispersion stabilities [7,8].

Indeed, the presence of such multivalent metal ions considerably influences the adsorption properties of the dispersant. Previous studies on the effects of multivalent metal ions on adsorption have shown that divalent ions can enhance the adsorption of polyacrylic acid (PAA) on alumina surfaces [9–12]. This effect, which is minimal under acidic conditions but pronounced under alkaline conditions [11], can be attributed to ion interactions, such as counterion screening or ion bridging, that reduce the electrostatic repulsion between polymer molecules to promote flocculation [13]. Furthermore, several recent studies [8,14] considered bulk particle behaviour to investigate the rheological properties of slurries and demonstrated that the addition of metal ions to slurries containing charged polymer dispersants promotes particle aggregation, increasing the slurry yield stress and decreasing its packing fraction.

The interactions between particle surfaces in the presence of adsorbed charged polymers have been actively investigated since the early use of AFM and SFA [15,16]. Direct measurements of these interactions have informed a comprehensive understanding of the behaviours of polyelectrolyte layers adsorbed on oppositely charged surfaces [17]. Kamiya's group [18,19] used AFM measurements to examine the relationship between the interaction forces on ceramic surfaces in the presence of dispersant polymers and evaluated the dispersibility of ceramic suspensions prepared using various solvents. Their findings revealed that interaction force significantly affected the fluidic properties of bulk suspensions. In particular, the gelation of the suspension correlated well with the occurrence of long-range attractive interactions between particles. Although the effects of multivalent ions have been investigated using SFA measurements of surfaces with tethered polyelectrolyte brushes [20,21], studies investigating the influences of ions on the interactions between surfaces with adsorbed polymers remain relatively limited.

Therefore, this study used AFM to directly measure the interaction forces between alumina surfaces in aqueous solutions with different concentrations of PAA, a commonly used dispersant, in the presence of different concentrations of metal ions to systemically investigate the effects of PAA adsorption as well as the resulting nanoscale structures formed on the alumina surfaces.

2. Materials and Methods

2.1. Materials

Reagent-grade PAA with an average molecular weight of 25,000 Da was purchased from Fujifilm Wako Pure Chemicals, Japan and used without further purification. Analytical-grade sodium chloride (NaCl), magnesium chloride ($MgCl_2$), and aluminium chloride ($AlCl_3$) were obtained from Fujifilm Wako Pure Chemical Industries, Japan and used as electrolytes without further treatment. All aqueous solutions were prepared using ultrapure water obtained from a Milli-Q system (Merck, Japan).

Spherical alumina particles 4–12 μm in diameter (Nippon Steel Chemical and Material, Japan) and alumina substrates (Japan Fine Ceramics, Japan) were used to conduct force measurements. Alumina particles with an average diameter of 0.5 μm (AES12, Sumitomo Chemical Co. Ltd., Japan) were used for electrophoretic measurements. All alumina particles were washed by stirring them in warm ethanol for 10 min, then in a 5 vol% nitric acid (Fujifilm Wako Pure Chemical Industries, Japan) solution for another 10 min before rinsing them twice with warm ultrapure water and drying them under reduced pressure. The alumina substrates were ultrasonically cleaned with acetone (Nacalai Tesque, Japan) for 10 min, then with concentrated nitric acid (Fujifilm Wako Pure Chemical Industries, Japan) for 30 min before subjecting them to ultrasonication in ultrapure water for 30 min and drying them in a nitrogen gas atmosphere.

2.2. Interaction force measurements

This study measured the interaction forces between alumina surfaces and electrophoretic mobilities of alumina particles to evaluate the effects of dispersant adsorption and metal ions on nanoscale particle structures and behaviours.

The interaction forces between the particle (colloidal probe) and substrate were measured by AFM (Pico SPM, Molecular Imaging, United States) using silicon nitride probes with triangular cantilevers (NP-S, Nanosensors, Switzerland) in 0, 0.001, 0.01, 0.1, 1.0, and 10.0 g/L PAA solutions with 0.01, 0.01, and 0.1 M concentrations of NaCl, $MgCl_2$, or $AlCl_3$. The spring constant k of the cantilever was determined by measuring the resonance frequency of the probe [22]. The colloidal probe was prepared by attaching a cleaned alumina particle to the top of the AFM cantilever using epoxy resin (Epikote 1004, Shell, United States) under an optical microscope. The force measurements were performed using a Teflon fluid cell to obtain force curves after equilibration for 1 h while immersing the substrate in the desired solution. The typical velocity at which the probe approached and retracted from the substrate was set to 300 nm/s.

2.3. Electrophoretic mobility measurements

Electrophoretic mobility measurements of the alumina particles were performed using a zeta potential analyser (ELSZ, Otsuka Electronics Corp., Japan). A 0.01 vol% concentration of cleaned alumina particles was dispersed in each of the same PAA–electrolyte solutions used in the AFM experiments to determine their electrophoretic mobility values.

3. Results and Discussion

3.1. Effects of polymer concentration

Fig. 1a shows the force curves between alumina surfaces in aqueous solutions of PAA at various concentrations in the presence of 0.01 M NaCl. In the absence of PAA (0 g/L), the force curve exhibited long-range repulsion attributable to the electrostatic double-layer forces. At shorter separation distances, the probe jumped abruptly into contact with the substrate, as indicated by the arrow on the force curve, indicating the presence of strong attractive forces. This "jump-in" occurs because of the mechanical instability of the cantilever; the phenomenon takes place when the gradient of the interaction force with respect to separation exceeds the spring constant of the cantilever. This attractive force is attributed to the van der Waals interactions between the surfaces, and

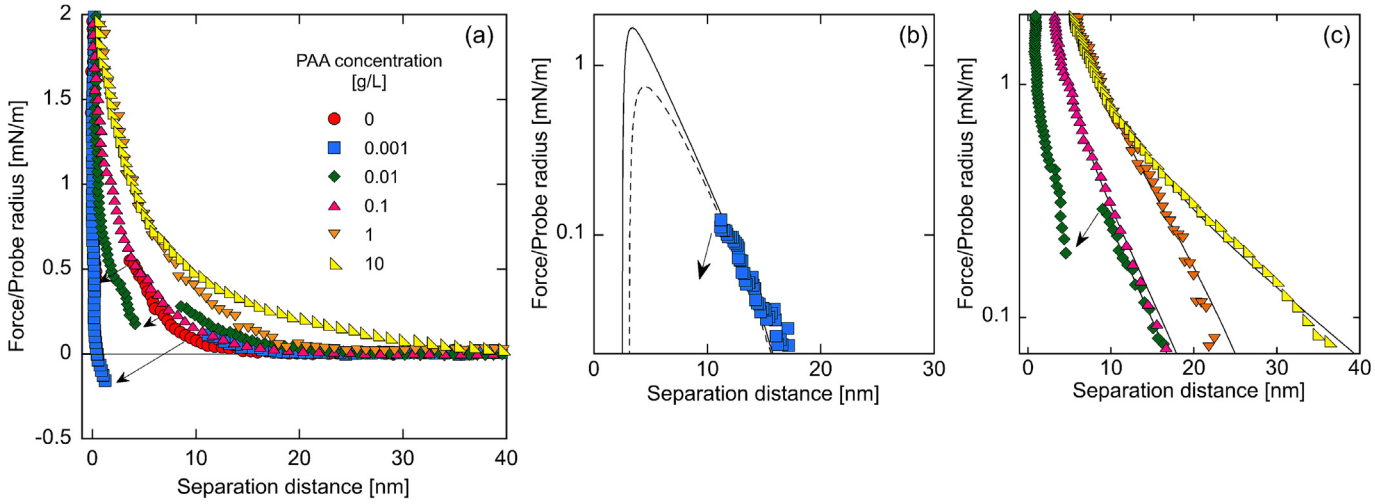

Fig. 1. (a) Force curves measured between alumina surfaces in PAA solutions of varying concentrations with 0.01 M NaCl. Arrows indicate jump-in of the surfaces. (b) Semi-logarithmic plot of the force curve for 0.001 g/L PAA fitted to DLVO theory using a surface potential of 40 mV and a Hamaker constant of 2.8×10^{-20} J. The solid and dashed lines indicate the DLVO theoretical curves under constant potential and charge conditions, respectively. (c) Semi-logarithmic plot of force curves for PAA concentrations ranging from 0.01 to 10 g/L fitted to AdG theory. Note that the point of zero distance is shifted using the calculated offset distance for each plot (Fig. 3b, 4b, 5b and 7b are also the same). The solid lines indicate AdG theoretical curves obtained using Eq. (1).

the overall force behaviour is well described by the DLVO theory. At low PAA concentrations (0.001 and 0.01 g/L), similar repulsive forces were observed at longer separation distances, followed by jump-ins, indicating that attractive forces were still present at short distances, as observed in the case of 0 g/L PAA. When the PAA concentration increased beyond 0.1 g/L, repulsion became dominant again, with the range of repulsive force extending as the concentration increased.

The applicability of DLVO theory to the force data in the presence of PAA was evaluated by fitting the experimentally obtained force curves to theoretical DLVO calculations. The DLVO calculations were performed by solving the nonlinear Poisson–Boltzmann equation under constant potential and charge boundary conditions using the algorithm proposed by Chan et al. [23] to determine the electrostatic double-layer force. The van der Waals (vdW) force was estimated assuming the Hamaker constant to be 2.8×10^{-20} J for alumina surfaces in water [24]. Note that an offset distance to the apparent zero separation was assumed to account for the presence of adsorbed PAA layers, which were expected to remain between alumina surfaces even at their closest approach.

Fig. 1b shows the best fit of the force curve to DLVO theory for the 0.001 g/L of PAA case using an assumed Debye length of 3.26 nm and an offset distance of 1.67 nm. This Debye length closely matched the theoretical value of 3.04 nm for an electrolyte concentration of 0.01 M, suggesting that double-layer repulsion primarily governed the interaction before the jump. However, the observed attractive force was longer-ranged than that predicted by the DLVO model, indicating that it was not caused by vdW forces.

At PAA concentrations exceeding 0.01 g/L, the observed repulsive force preceding the attractive interaction could not be adequately fitted to DLVO theory, suggesting that steric repulsion owing to the adsorbed PAA dominated at these concentrations. To verify this explanation, we also fitted the force curves to the Alexander–de Gennes (AdG) model [25], which describes the interactions between polymer brush layers under compression. According to this model, the force F between a flat plate and sphere of radius R separated by a distance D is given by [26,27]

$$\frac{F}{R} = \frac{16\pi k_B T L_0}{35 s^3}\left[7\left(\frac{2L_0}{D}\right)^{5/4} + 5\left(\frac{D}{2L_0}\right)^{7/4} - 12\right] \quad (1)$$

where L_0 is the uncompressed brush thickness, k_B is the Boltzmann constant, T is the temperature, and s is the average distance between adsorption points of the polymer on the surface. The fitting results were obtained by assuming offset distances using an approach similar to that used for DLVO fitting, and the variation in the thickness of the adsorbed PAA layer was estimated based on the L_0 values [27].

The resulting fitting curves in Fig. 1c agree well with the experimental data, confirming that the observed repulsive forces were indeed steric interactions between adsorbed polymers. These polymers formed brush-like layers on the alumina surfaces owing to chain expansion via loop and tail conformations. At a PAA concentration of 0.01 g/L, the fitted curve yielded estimated L_0 and offset values of 15.8 nm and 0.6 nm, respectively, suggesting that steric repulsion was the dominant force before the jump occurred at approximately 8 nm. The estimated L_0 values at PAA concentrations of 0.1, 1, and 10 g/L were 16.1, 19.0, and 41.8 nm, respectively. This increase in L_0 with increasing concentration suggests that a higher adsorption density promoted a more extended polymer conformation. We also note that the s values in Equation (1) were obtained as fitting parameters because the direct measurement of adsorption density on flat surfaces is difficult. The fitted s values ranged from 3.5 to 8.2 nm. Using the relationship $s = (\sigma/\pi)^{1/2}$, where σ is the surface area per polymer chain, we estimated the adsorption density to be between 0.2 and 1.1 mg/m^2. These values are in good agreement with those reported in previous studies [11,12,28] on PAA adsorption on alumina, indicating that the fitted s values fall within a reasonable and physically meaningful range.

The electrophoretic mobilities of the alumina particles in each solution evaluated in the AFM experiments are compared in Fig. 2. When no PAA was present, the zeta potential of the alumina particles was approximately + 55 mV, which is equivalent to a mobility of $+ 4.8 \times 10^{-8}$ m^{2}V^{-1}s^{-1} (not shown in Fig. 2). The mobility was lower in 0.001 g/L of PAA owing to the adsorption of the negatively charged PAA, and charge reversal was observed on the particle surface in 0.01 g/L of PAA, suggesting that 0.01 M NaCl was insufficient to fully neutralize the surface charge even at this low polymer concentration. Increases in the PAA concentration to 1 g/L and 10 g/L further decreased the mobility. The pH value decreased with increasing PAA concentration, reaching 3.3 at

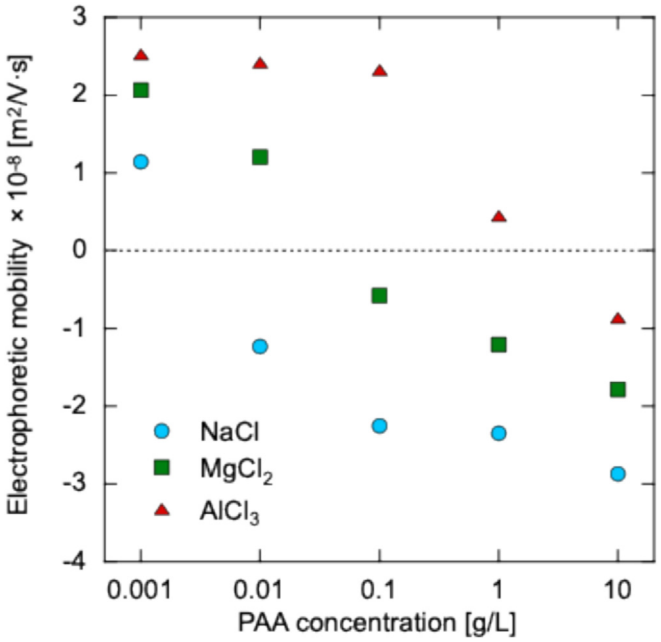

Fig. 2. Electrophoretic mobilities of alumina particles dispersed in PAA solutions of various concentrations in the presence of 0.01 M NaCl, $MgCl_2$, or $AlCl_3$.

1 g/L and 2.9 at 10 g/L. Previous studies have shown that a lower pH results in higher adsorption [28] although the degree of dissociation of the carboxyl groups decreases. Therefore, the more negative mobility with increasing PAA concentration is likely to be caused by a higher negative charge density owing to the increased adsorption of PAA on the particle surface.

Based on these results, the following common mechanism for surfaces in adsorptive polymer solutions [29,30] can be applied to explain the observed interactions in the presence of monovalent NaCl. At a PAA concentration of 0.001 g/L, the adsorption density on the alumina surface should be sufficiently low (based on the positive electrophoretic mobility value) that the polymer chains adsorbed on one surface can extend and bridge to the opposite surface, generating the attractive force observed at a separation of 10 nm, which was strong enough to overcome electrostatic repulsion. Similarly, the attractive force observed at 0.01 g/L was likely generated by bridging interactions, although weak repulsion was observed before attraction owing to the steric force induced by the increasing density of adsorbed polymers [31]. As the PAA concentration increased further, greater quantities of PAA were adsorbed onto the alumina surfaces, making steric repulsion dominant and extending its range via the formation of thicker and more concentrated adsorbed PAA layers.

Fig. 3 shows the force curves obtained when the $MgCl_2$ was used. The interaction forces transitioned from repulsive to attractive at lower PAA concentrations, and the repulsive forces became shorter than those observed for the NaCl at PAA higher concentrations. No repulsive forces were detected at PAA concentrations of 0.001 and 0.01 g/L, and only an attractive force comparable to the vdW force was observed. This indicates that the higher ionic strength of Mg^{2+} than Na^+ enhanced electrostatic screening, effectively suppressing electrostatic repulsion and allowing vdW attraction to dominate at these concentrations. The absence of the attraction longer than vdW, as observed for NaCl, was likely a result of the stronger screening effect of $MgCl_2$, which reduced polymer extension and bridging interactions. This screening of $MgCl_2$ can also be inferred from the electrophoretic mobility values shown in Fig. 2, which shifted to larger positive values than those observed for the NaCl electrolyte.

The repulsive forces for the 1 and 10 g/L PAA concentration $MgCl_2$ solutions exhibited shorter ranges than those for the equivalent NaCl solutions. Furthermore, the AdG equation did not fit the theoretical values at 1 g/L. The low electrophoretic mobility at this concentration suggests that the PAA molecules adopted a globular state because of strong screening. However, the repulsive forces for the 10 g/L PAA concentration exhibited suitable fit to the AdG equation, giving an L_0 value of 31.4 nm with an s value of 4.5 nm, which is 25 % shorter than that measured for the NaCl solution at the same concentration. This indicates that $MgCl_2$ screening was no longer sufficient at this concentration because of the greater quantities of PAA adsorbed onto the alumina surface despite the presence of more collapsed PAA molecule brush structures than in the NaCl solution, resulting in a reduced layer thickness.

This was quite pronounced when trivalent $AlCl_3$ was used as the electrolyte, as shown in Fig. 4. The force curves measured at PAA concentrations up to 1 g/L exhibited attraction within the range of vdW interactions, suggesting conformational collapse of the PAA even at low concentrations. This occurred despite the relatively high surface potentials, suggested by the electrophoretic mobilities as shown in Fig. 2, observed at PAA concentrations up to 0.1 g/L. Indeed PAA–Al^{3+} complexes are likely to form in the presence of $AlCl_3$, leading to the aggregation of PAA on the alumina surface. Thus, the positive electrophoretic mobilities observed in this concentration range can be attributed to the excess charge carried by bound Al^{3+} ions.

At a PAA concentration of 10 g/L, the force was monotonically repulsive over a considerably shorter range for the $AlCl_3$ electrolyte than for the NaCl or $MgCl_2$ electrolytes. This repulsive force also fit the AdG equation well with an L_0 value of 5.88 nm and an s value of 3.8 nm, which is much shorter than those for the NaCl and $MgCl_2$ solutions at the same concentrations. This reduction indicates that the PAA molecules underwent greater collapse while maintaining a brush-like molecular conformation, presumably because the screening and/or formation of PAA–Al^{3+} complexes was insufficient owing to the greater quantity of PAA adsorption.

These changes in the interaction forces, which depend on the valence and concentration of ions, can be qualitatively correlated with the dispersion behaviour of the bulk alumina particles. Nakamura et al. [8] measured the viscosity of alumina slurries in polycarboxylic acid ammonium (PCA) solutions in the presence of Mg^{2+} or Al^{3+} ions and found that the presence of 0.01 M of either of these ions increased the viscosity of the slurry when the PCA concentration was relatively low, but the viscosity decreased again when the PCA concentration increased. Although there are indeed differences between PCA and PAA, both are anionic polymers, suggesting that the attraction between particles tends to increase as the ion valence and concentration increase, enhancing particle aggregation and increasing viscosity. Furthermore, the improved dispersion and decreased viscosity observed at higher polymer concentrations can be considered a result of repulsion owing to insufficient ion screening, as observed in the present experiment.

3.2. Effects of electrolyte concentration

The effect of NaCl concentration on the measured interaction forces was examined for a fixed PAA concentration of 1 g/L while varying the NaCl concentration from 0.001 to 0.1 M. As shown in Fig. 5, when the NaCl concentration ranged from 0.001 to 0.1 M under these conditions, steric repulsion dominated the interactions and the repulsive forces did not fit DLVO theory, but were effectively described by the AdG model, as shown in Fig. 5b. The decreasing range of repulsive forces with increasing NaCl concentration indicates the collapse of adsorbed PAA chains owing to electrostatic screening, although the brush conformation contin-

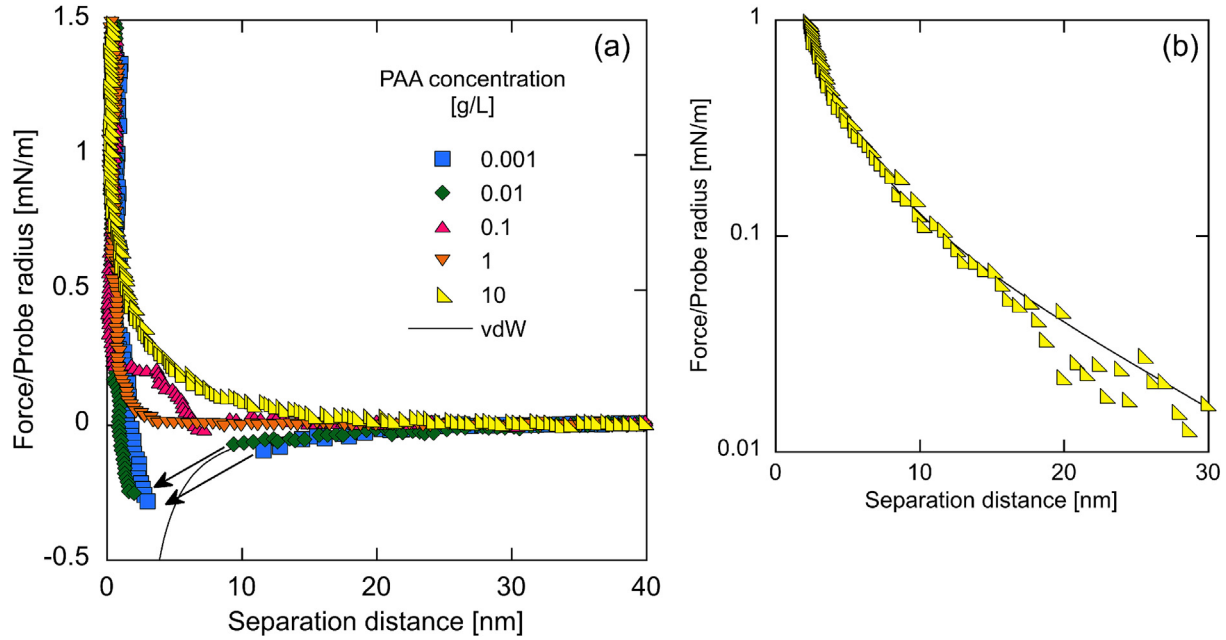

Fig. 3. (a) Force curves measured between alumina surfaces in PAA solutions of varying concentrations with 0.01 M $MgCl_2$. Arrows indicate jump-in of the surfaces. (b) Semi-logarithmic plot of the force curve for 10 g/L PAA fitted to AdG theory. The solid line indicates the AdG theoretical curve obtained using Eq. (1).

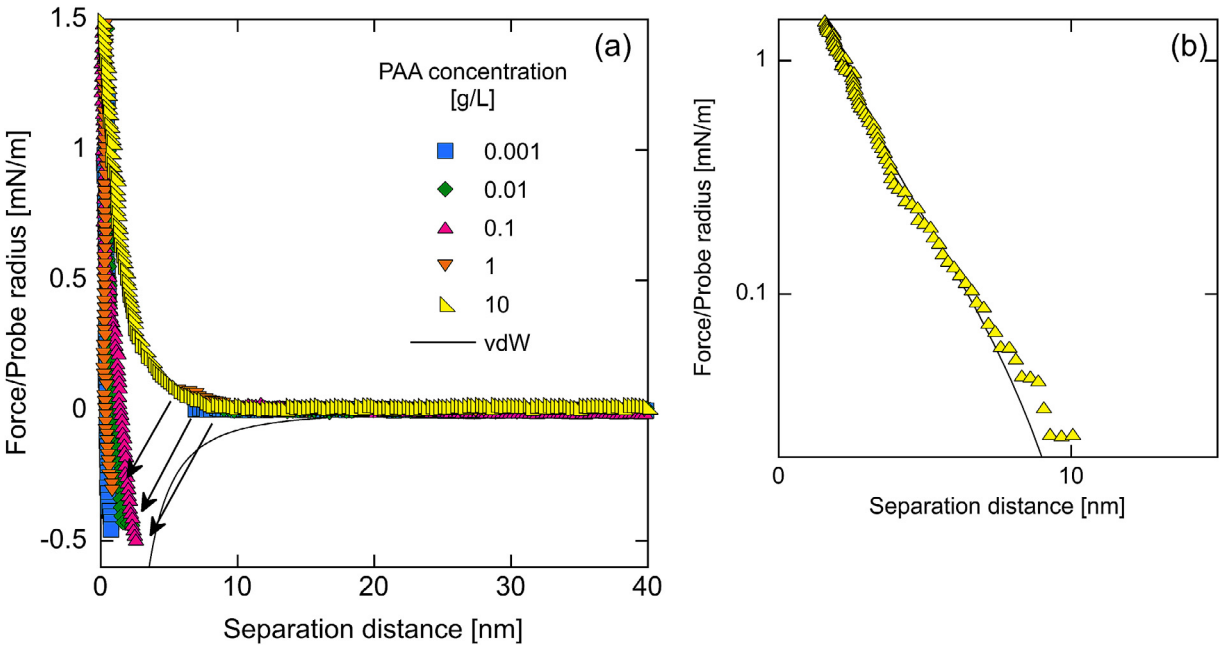

Fig. 4. (a) Force curves measured between alumina surfaces in PAA solutions of varying concentrations with 0.01 M $AlCl_3$. Arrows indicate jump-in of the surfaces. (b) Semi-logarithmic plot of the force curve for 10 g/L PAA fitted to AdG theory. The solid line indicates the AdG theoretical curve obtained using Eq. (1).

ued up to a 0.1 M NaCl concentration. Critically, no attractive force was observed in this concentration range, suggesting that a 0.1 M NaCl electrolyte concentration was insufficient to screen the charge of adsorbed PAA molecules. These forces corresponded well with the electrophoretic mobility data shown in Fig. 6, the absolute value of which decreased with increasing NaCl concentration, suggesting that electrostatic screening induced polymer chain collapse, thereby reducing the range of steric repulsion.

The overall force curve trends for the different $MgCl_2$ concentrations exhibited stronger screening effects than those for the different NaCl concentrations, as shown in Fig. 7. The range of repulsive forces decreased at 0.001 and 0.01 M, and an attractive force was already observed at 0.1 M, suggesting enhanced charge screening by divalent Mg^{2+} ions. The absolute value of electrophoretic mobility in the $MgCl_2$ solution, shown in Fig. 6, was also lower than that in the NaCl solution, indicating enhanced polymer collapse and, consequently, shorter-range forces.

Finally, the forces for the different $AlCl_3$ concentrations are shown in Fig. 8. The repulsive force was apparent at 0.001 M $AlCl_3$, but its range was much smaller than those of the other electrolytes at the same concentration. The vdW attraction appeared to have overcome the steric repulsion at 0.01 M $AlCl_3$; these attractive ten-

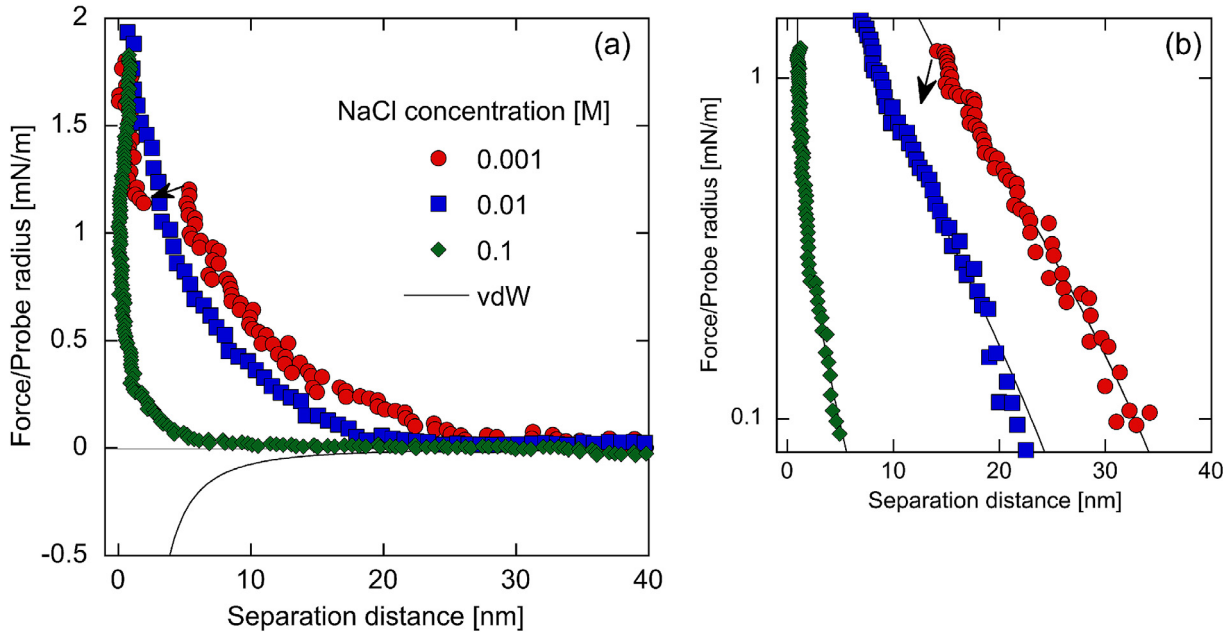

Fig. 5. (a) Force curves measured between alumina surfaces in 1 g/L PAA solutions with NaCl at varying concentrations. Arrow indicates jump-in of the surfaces. (b) Semi-logarithmic plot of the force curves fitted to AdG theory. The solid lines indicate AdG theoretical curves obtained using Eq. (1).

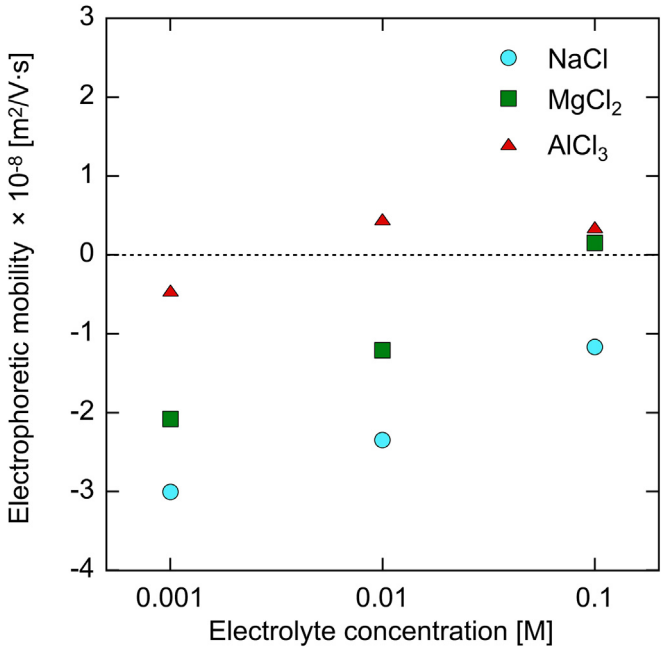

Fig. 6. Electrophoretic mobilities of the alumina particle dispersed in 1 g/L PAA solutions with the various concentration of NaCl, $MgCl_2$, and $AlCl_3$.

dencies were likely caused by strong screening by Al^{3+} ions, as indicated by the low electrophoretic mobilities shown for $AlCl_3$ in Fig. 6. Notably, an anomalous long-range attractive force was observed at a distance of approximately 20 nm in the 0.1 M solution. This force was significantly longer-ranged than the vdW force, which differs markedly from the results obtained for other electrolytes.

Determining the origin of this long-range attractive interaction is difficult at present. Polymer bridging is unlikely under high-ionic-strength conditions because the polymer chains are expected to exhibit strongly collapsed conformations. Instead, a possible mechanism to be considered is that the interaction caused by patchy charge domains of PAA molecules [32,33]. In polyelectrolyte solutions, the origin of attractive forces greater than the vdW attraction is often attributed to charge patches along with polymer bridging [33]. These patches occur when polyelectrolytes are adsorbed on a surface forming domains and creating an uneven charge distribution [34]. The adsorbed and oppositely charged non-adsorbed regions electrostatically attract each other, producing long-range attraction. This phenomenon has been observed not only on polymer-adsorbed surfaces but also on surfactant- or amphiphile-adsorbed ones, where it represents a cause of strong attraction between surfaces hydrophobized by such molecules [35,36].

In the present case, the high ionic strength of Al^{3+} in the solution likely led to strong screening and ion binding between the PAA molecules, causing them to form compact domains. However, because many counterions can be adsorbed onto the alumina surface, the non-adsorbed regions of the screened surface likely remained negatively charged. Therefore, under the present conditions, the possibility that charge patches are the primary cause of attraction appears low.

Another possibility is the underscreening effect that arises in solutions with high ionic strengths. Recent studies have shown that the classical Debye–Hückel theory, which describes electrostatic screening lengths, is inadequate at high electrolyte concentrations [37]. Specifically, for electrostatic interactions between charged macroscopic surfaces, the decay length of the repulsive force exceeds the Debye length beyond a certain electrolyte concentration—typically approximately 0.5–1 M for monovalent electrolytes—increasing the range of electrostatic interactions [38]. This phenomenon, known as underscreening, has been observed in SFA measurements when the electrostatic decay lengths in various electrolyte solutions, including ionic liquids, deviate from classical predictions [39–41].

Underscreening also occurs with ionic polymers in highly concentrated salt solutions. Roiter et al. [42] demonstrated that poly (2-vinylpyridine) polymer coils re-expanded in solutions with high salt concentrations to exhibit radii of gyration comparable to those in dilute solutions. Furthermore, Robertson et al. [43] measured

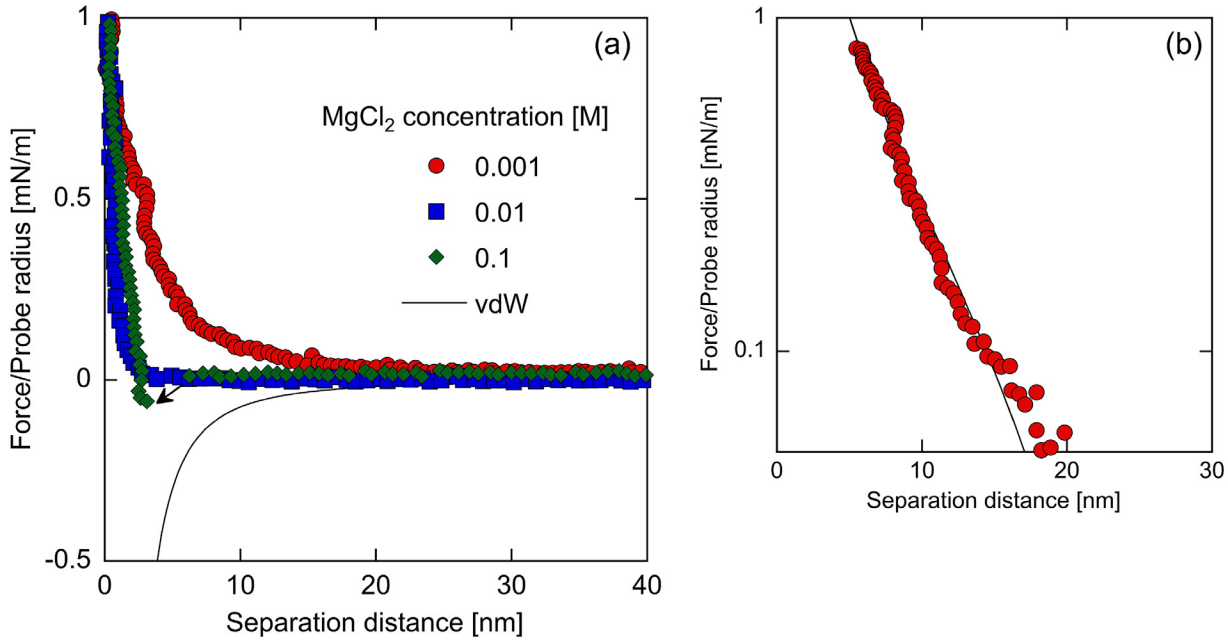

Fig. 7. (a) Force curves force curves measured between alumina surfaces in 1 g/L PAA solutions with $MgCl_2$ at varying concentrations. Arrow indicates jump-in of the surfaces. (b) Semi-logarithmic plot of the force curve for $MgCl_2$ concentration of 0.001 M, fitted to the AdG theory. Solid lines indicate AdG theoretical curves obtained using Eq. (1).

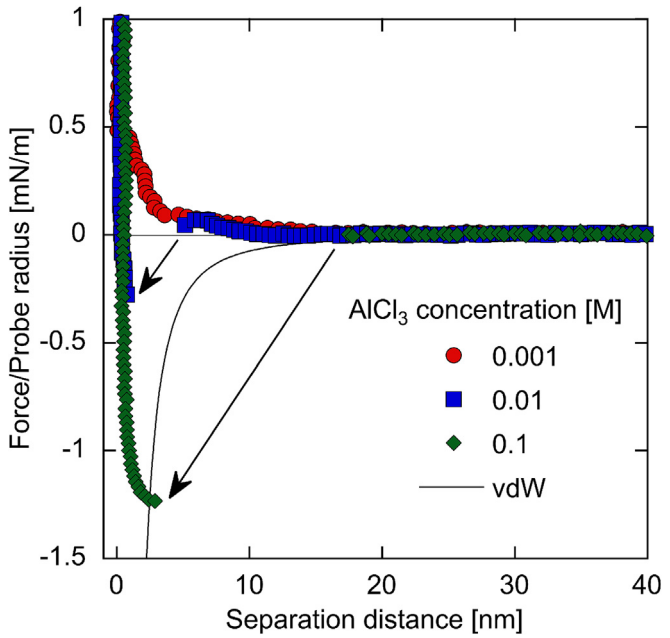

Fig. 8. Force curves measured between alumina surfaces in 1 g/L PAA solutions with $AlCl_3$ at varying concentrations. Arrows indicate jump-in of the surfaces.

the thickness of substrate-tethered poly(2-(methacryloyloxy)ethyl)trimethylammonium brushes and observed re-entrant swelling in multivalent electrolyte solutions with high concentrations. They also suggested that this re-entrant swelling was consistent with the underscreening effect observed on solid surfaces.

A similar polymer re-expansion is highly likely to have occurred in this study. If such re-expanded PAA molecules form bridges between alumina surfaces, they could induce long-range attraction. However, for this bridging to occur, PAA, which is expected to be positively charged owing to Al^{3+} adsorption, must be adsorbed onto the opposing surface. Because the alumina surface is positively charged, the possibility of PAA chains adsorbing onto the non-adsorbed regions of the opposing alumina surface remains low even if the PAA retains some localised negative regions, as in the case of patchy surface charges. Thus, underscreening alone does not appear sufficient to explain the origin of this anomalous attraction, and a more comprehensive investigation remains required accordingly.

4. Conclusions

This study used AFM to investigate the interaction forces between alumina surfaces in PAA solutions containing different metal ions. In the presence of NaCl, attractive forces dominated at low PAA concentrations owing to polymer bridging, whereas steric repulsion between PAA chains became dominant at higher concentrations, as is commonly observed in adsorptive polymer systems. In contrast, the presence of $MgCl_2$ and $AlCl_3$ resulted in increasingly attractive interactions. This trend was attributed to two primary effects: enhanced electrostatic screening of the negatively charged PAA by divalent and trivalent metal ions, which reduced the range of electrostatic repulsion, and PAA chain collapse, which minimised steric repulsion. These changes in the interaction forces qualitatively explain the dispersion behaviours of bulk alumina particles in the presence of $MgCl_2$ and $AlCl_3$. Similarly, increasing the concentration of these metal ions further reduced the repulsive forces, eventually resulting in a net attraction driven by the same electrostatic screening and polymer collapse mechanisms. At 0.1 M $AlCl_3$, a specific attractive force longer than vdW attraction emerged that was not observed in the presence of NaCl or $MgCl_2$. However, further research is required to confirm the mechanism of this unique interaction force.

In this study, we conducted measurements at ion concentrations higher than those commonly used in industrial processes. Because our aim was to evaluate the effects of metal ions on the adsorption and interactions of PAA, this approach can systematically explain how such interactions vary with ion concentration, which is also important for considering the particle behaviour in

the bulk phase. Thus, we believe that the results of this study can improve the control of ceramic slurry dispersion at the microscopic level to ensure consistency in the quality of manufactured ceramics.

CRediT authorship contribution statement

Naoto Kishimoto: Investigation, Data curation. **Ryota Kaji:** Investigation, Data curation. **Katsumi Tsuchiya:** Writing – review & editing. **Koreyoshi Imamura:** Writing – review & editing, Supervision. **Naoyuki Ishida:** Writing – review & editing, Writing – original draft, Supervision, Project administration, Funding acquisition, Data curation, Conceptualization.

Declaration of competing interest

The authors declare that they have no known competing financial interests or personal relationships that could have appeared to influence the work reported in this paper.

Acknowledgments

N.I. acknowledges the financial support of the Adaptable and Seamless Technology Transfer Program, Target-driven R (A-STEP) Stage I, from the Japan Science and Technology Agency (JST), and the research grant from the Information Center of Particle Technology, Japan.

References

[1] B.V. Derjaguin, L.D. Landau, Theory of the stability of strongly charged lyophobic sols and of the adhesion of strongly charged particles in solution of electrolytes, Acta Physicochim. URSS 14 (1941) 633–662.
[2] E.J.W. Verwey, J.T.G. Overbeek, Theory of the Stability of Lyophobic Colloids, Elsevier, Amsterdam, 1948.
[3] J.N. Israelachvili, G.E. Adams, Measurement of forces between two mica surfaces in aqueous electrolyte solutions in the range 0-100 nm, J. Chem. Soc. Faraday Trans. 1 (74) (1978) 975–1001.
[4] H.-J. Butt, Measuring electrostatic, van der Waals, and hydration forces in electrolyte solutions with an atomic force microscope, Biophys. J . 60 (1991) 1438–1444.
[5] W.A. Ducker, T.J. Senden, R.M. Pashley, Direct measurement of colloidal forces using an atomic force microscope, Nature 353 (1991) 239–241.
[6] N. Ishida, V.S.J. Craig, Direct Measurement of Interaction Forces between Surfaces in Liquids using Atomic Force Microscopy, Kona Powder Part. J. 36 (2019) 187–200.
[7] H. Ohtsuka, H. Mizutani, S. Iio, K. Asai, T. Kiguchi, H. Satone, T. Mori, J. Tsubaki, Effects of sintering additives on dispersion properties of Al_2O_3 slurry containing polyacrylic acid dispersant, J. Eur. Ceram. Soc. 31 (2011) 517–522.
[8] K. Nakamura, N. Iwata, T. Mori, Effects of eluted metal ions on the properties of ceramic slurry and slip-casted green bodies, J. Asian Ceram. Soc. 8 (2020) 528–536.
[9] E. Ringenbach, G. Chauveteau, E. Pefferkorn, Effect of soluble aluminum ions on polyelectrolyte-alumina interaction. Kinetics of polymer adsorption and colloid stabilization, Colloids Surf. A 99 (1995) 161–173.
[10] L. Dupont, A. Foissy, R. Mercier, B. Mottet, Effect of Calcium Ions on the Adsorption of Polyacrylic Acid onto Alumina, J. Colloid Interface Sci. 161 (1993) 455–464.
[11] J. Sun, L. Bergström, L. Gao, Effect of Magnesium Ions on the Adsorption of Poly (acrylic acid) onto Alumina, J. Am. Ceram. Soc. 84 (2001) 2710–2712.
[12] K. Vermöhlen, H. Lewandowski, H.D. Narres, M.J. Schwuger, Adsorption of polyelectrolytes onto oxides — the influence of ionic strength, molar mass, and Ca^{2+} ions, Colloids Surf, A 163 (2000) 45–53.
[13] G.H. Kirby, D.J. Harris, Q. Li, J.A. Lewis, Poly(acrylic acid)–Poly(ethylene oxide) Comb Polymer Effects on $BaTiO_3$ Nanoparticle Suspension Stability, J. Am. Ceram. Soc. 87 (2004) 181–186.
[14] H. Satone, K. Iimura, N. Minami, A. Nasu, Effect of Multivalent Ions on Ionic Crosslinking of Polyelectrolytes Adsorbed on Particle, J. Soc. Powder Technol., Jpn 56 (2019) 496–500.
[15] P.F. Luckham, J. Klein, Forces between mica surfaces bearing adsorbed polyelectrolyte, poly-L-lysine, in aqueous media, J. Chem. Soc. Faraday Trans. 1 (80) (1984) 865–878.
[16] S. Biggs, A.D. Proud, Forces between Silica Surfaces in Aqueous Solutions of a Weak Polyelectrolyte, Langmuir 13 (1997) 7202–7210.
[17] P.M. Claesson, E. Poptoshev, E. Blomberg, A. Dedinaite, Polyelectrolyte-mediated surface interactions, Adv. Colloid Interface Sci. 114–115 (2005) 173–187.
[18] M. Yamamoto, S. Shimai, K. Oguma, S. Wang, H. Kamiya, Alumina particle surface interaction in copolymer of isobutylene and maleic anhydride aqueous solution characterized by colloidal probe atomic force microscopy, Powder Technol. 354 (2019) 369–376.
[19] T. Kakui, T. Miyauchi, H. Kamiya, Analysis of the action mechanism of polymer dispersant on dense ethanol alumina suspension using colloidal probe AFM, J. Eur. Ceram. Soc. 25 (2005) 655–661.
[20] R. Farina, N. Laugel, P. Pincus, M. Tirrell, Brushes of strong polyelectrolytes in mixed mono- and tri-valent ionic media at fixed total ionic strengths, Soft Matter 9 (2013) 10458–10472.
[21] J. Yu, J. Mao, G. Yuan, S. Satija, Z. Jiang, W. Chen, M. Tirrell, Structure of Polyelectrolyte Brushes in the Presence of Multivalent Counterions, Macromolecules 49 (2016) 5609–5617.
[22] J.P. Cleveland, S. Manne, D. Bocek, P.K. Hansma, A nondestructive method for determining the spring constant of cantilevers for scanning force microscopy, Rev. Sci. Instrum. 64 (1993) 403–405.
[23] D.Y.C. Chan, R.M. Pashley, L.R. White, A simple algorithm for the calculation of the electrostatic repulsion between identical charged surfaces in electrolyte, J. Colloid Interface Sci. 77 (1980) 283–285.
[24] J.N. Israelachvili, Intermolecular and Surface Forces, Third Edition., Academic Press, San Diego, 2011.
[25] P.G. de Gennes, Conformations of Polymers Attached to an Interface, Macromolecules 13 (1980) 1069–1075.
[26] S. Block, C.A. Helm, Conformation of Poly(styrene sulfonate) Layers Physisorbed from High Salt solution Studied by Force Measurements on two Different Length Scales, J. Phys. Chem. B 112 (2008) 9318–9327.
[27] S.C. McLean, H. Lioe, L. Meagher, V.S.J. Craig, M.L. Gee, Atomic Force Microscopy Study of the Interaction between Adsorbed Poly(ethylene oxide) Layers: Effects of Surface Modification and Approach Velocity, Langmuir 21 (2005) 2199–2208.
[28] M. Wiśniewska, T. Urban, E. Grządka, V.I. Zarko, V.M. Gun'ko, Comparison of adsorption affinity of polyacrylic acid for surfaces of mixed silica–alumina, Colloid. Polym. Sci., 292 (2014) 699-705.
[29] Y. Zhou, Y. Gan, E.J. Wanless, G.J. Jameson, G.V. Franks, Interaction Forces between Silica Surfaces in Aqueous Solutions of Cationic Polymeric Flocculants: effect of Polymer Charge, Langmuir 24 (2008) 10920–10928.
[30] M.A.G. Dahlgren, A. Waltermo, E. Blomberg, P.M. Claesson, L. Sjoestroem, T. Aakesson, B. Joensson, Salt effects on the interaction between adsorbed cationic polyelectrolyte layers: theory and experiment, J. Phys. Chem. 97 (1993) 11769–11775.
[31] S. Fujii, M. Suzaki, Y. Nakamura, K. Sakai, N. Ishida, S. Biggs, Surface characterization of nanoparticles carrying pH-responsive polymer hair, Polymer 51 (2010) 6240–6247.
[32] M. Borkovec, G. Papastavrou, Interactions between solid surfaces with adsorbed polyelectrolytes of opposite charge, Curr. Opin. Colloid Interface Sci. 13 (2008) 429–437.
[33] M. Borkovec, I. Szilagyi, I. Popa, M. Finessi, P. Sinha, P. Maroni, G. Papastavrou, Investigating forces between charged particles in the presence of oppositely charged polyelectrolytes with the multi-particle colloidal probe technique, Adv. Colloid Interface Sci. 179–182 (2012) 85–98.
[34] L.J. Kirwan, G. Papastavrou, M. Borkovec, S.H. Behrens, Imaging the Coil-to-Globule Conformational transition of a Weak Polyelectrolyte by Tuning the Polyelectrolyte Charge Density, Nano Lett. 4 (2004) 149–152.
[35] J. Zhang, R.-H. Yoon, M. Mao, W.A. Ducker, Effects of Degassing and Ionic Strength on AFM Force Measurements in Octadecyltrimethylammonium Chloride Solutions, Langmuir 21 (2005) 5831–5841.
[36] E.E. Meyer, K.J. Rosenberg, J. Israelachvili, Recent progress in understanding hydrophobic interactions, Proc. Natl. Acad. Sci. U.S.A. 103 (2006) 15739–15746.
[37] H. Yuan, W. Deng, X. Zhu, G. Liu, V.S.J. Craig, Colloidal Systems in Concentrated Electrolyte Solutions Exhibit Re-entrant Long-Range Electrostatic Interactions due to Underscreening, Langmuir 38 (2022) 6164–6173.
[38] A.A. Lee, C.S. Perez-Martinez, A.M. Smith, S. Perkin, Underscreening in concentrated electrolytes, Faraday Discuss. 199 (2017) 239–259.
[39] M.A. Gebbie, H.A. Dobbs, M. Valtiner, J.N. Israelachvili, Long-range electrostatic screening in ionic liquids, Proc. Natl. Acad. Sci. U.S.A. 112 (2015) 7432–7437.
[40] A.A. Lee, C.S. Perez-Martinez, A.M. Smith, S. Perkin, Scaling Analysis of the Screening Length in Concentrated Electrolytes, Phys. Rev. Lett. 119 (2017) 026002.
[41] A.M. Smith, A.A. Lee, S. Perkin, The Electrostatic Screening Length in Concentrated Electrolytes increases with Concentration, J. Phys. Chem. Lett. 7 (2016) 2157–2163.
[42] Y. Roiter, O. Trotsenko, V. Tokarev, S. Minko, Single Molecule Experiments Visualizing Adsorbed Polyelectrolyte Molecules in the Full Range of Mono- and Divalent Counterion Concentrations, J. Am. Chem. Soc. 132 (2010) 13660–13662.
[43] H. Robertson, G.R. Elliott, A.R.J. Nelson, A.P. Le Brun, G.B. Webber, S.W. Prescott, V.S.J. Craig, E.J. Wanless, J.D. Willott, Underscreening in concentrated electrolytes: re-entrant swelling in polyelectrolyte brushes, Phys. Chem. Chem. Phys. 25 (2023) 24770–24782.